Optimized Parallel Transmission in Elastic Optical Networks to Support High-Speed Ethernet

Xiaomin Chen, Admela Jukan, and Ashwin Gumaste

Abstract—**The need for *optical parallelization* is driven by the imminent *optical capacity crunch*, where the spectral efficiency required in the coming decades will be beyond the Shannon limit. To this end, the emerging high-speed Ethernet services at 100 Gbps have already standardized options to utilize parallel optics for data transmission, referred to as *multi-lane distribution*. OFDM-based optical network is a promising transmission option towards the goal of Ethernet parallelization. It can allocate optical spectrum resource tailored for a variety of bandwidth requirements in a fundamentally parallel fashion, with each sub-carrier utilizing a frequency slot at a lower rate than if serial transmission is used. In this paper, we propose a novel parallel transmission framework designed for elastic (OFDM-based) optical networks to support high-speed Ethernet services, in-line with IEEE and ITU-T standards. We formulate an optimization model based on integer linear programming, with consideration of various constraints, including spectrum fragmentation, differential delay and guard-band constraints. We also propose a heuristic algorithm which can be applied when the optimization model becomes intractable. The numerical results show the effectiveness and high suitability of elastic optical networks to support high-speed Ethernet parallel transmission, especially for connections with high bandwidth requirements. To the best of our knowledge, this is the first attempt to model parallel transmission in elastic optical networks in support of a standardized high-speed Ethernet system.**

Index Terms—**Elastic optical networks, high-speed ethernet, optical parallel transmission.**

I. Introduction

THE need for *optical parallelization* is driven by the imminent *optical capacity crunch* [1], which has gained significant attention after studies showed that capacity upgrades of conventional single-mode fiber (SMF) systems have slowed down from about 80% per year to about 20% per year since 2002 [1]. Given the massive growth of Internet traffic, it became clear that optical communications had to shift towards high spectral efficiency, i.e., transmitting more information over the fundamentally limited bandwidth of optical amplifiers. It has also become apparent that without parallelization, the spectral efficiency of about 20 b/s/Hz required in the coming decades, will be beyond the Shannon limit [1]. As a consequence, the high-speed Ethernet has resorted to a parallel solution as standardized in IEEE 802.3ba, especially for 40/100 Gigabit Ethernet (40/100 GE) and beyond, to overcome the Shannon limit without an expense on reduced transmission distance. Instead of using high-speed serial interfaces, 40 GE and 100 GE utilize parallel optics to split traffic across multiple lanes with lower rates, which is referred to as *multi-lane distribution* (MLD) [2]. To this end, it has been specified that 40 GE and 100 GE can utilize four and ten parallel lanes, respectively, with each lane running at 10.3125 Gbps [2]. In addition, ITU-T has extended the optical transport network (OTN) information structure for 40 GE and 100 GE. As it is, the concept of parallel transmission for high-speed Ethernet presents a myriad of new challenges in the optical layer.

We believe that recently proposed elastic optical networks based on orthogonal frequency division multiplexing (OFDM) technology carry the promise of a potentially transformative transmission solution for high-speed Ethernet, due to its fundamentally parallel nature. With OFDM, optical spectrum is actually *sliced or parallelized* into a sequence of frequency slots and signals are modulated on frequency slots in form of sub-carriers. Since the sub-carriers are orthogonal in the frequency domain, they can be received in parallel without interference. Hence, the OFDM-based elastic optical networks can efficiently support high-speed Ethernet parallel transmission and can also take full advantage of optical virtual concatenation (OVC) protocol in OTN, with parallel transmission over multiple spectrum paths in OFDM networks and each spectrum path composed of a group of consecutive sub-carriers.[1] At the same time, parallel transmission can alleviate the fundamental trade-off between bit rate and the optical reach, by using multiple low-speed spectrum paths. As it is well-known that imperfections in the optical fibers, such as transmission loss, non-linear effects, group velocity dispersion (GVD), and polarization mode dispersion, lessen with the decreased serial bit rate per connection.

Fig. 1 presents the detailed scheme of a 100 GE example on the transmitter side. Spectrum on each fiber is *sliced* or, as we refer to as *parallelized*, into ten frequency slots (dashed lines denote the existing sub-carriers). OTN layer acts as an adaptation layer, mapping the Ethernet traffic onto sub-carriers. To illustrate role of the OTN layer and without loss of generality, we show an asymmetric mapping between Ethernet lanes and sub-carriers. Currently, IEEE 802.3ba specifies two schemes for

Manuscript received June 22, 2013; revised September 12, 2013 and November 8, 2013; accepted November 08, 2013. Date of publication November 13, 2013; date of current version December 11, 2013.

X. Chen and A. Jukan are with the Technische Universität Carolo-Wilhelmina zu Braunschweig, 38106 Brunswick, Germany (e-mail: chen@ida.ing.tu-bs.de; jukan@ida.ing.tu-bs.de).

A. Gumaste is with the Department of Computer Science and Engineering, Indian Institute of Technology Bombay, Mumbai 400076, India (e-mail: ashwing@ieee.org).

Color versions of one or more of the figures in this paper are available online at http://ieeexplore.ieee.org.

Digital Object Identifier 10.1109/JLT.2013.2291318

[1]With OVC protocol, m Ethernet lanes are carried by n sub-carriers as though they were virtually contiguous. The number of sub-carriers (n) depends on the capacity of sub-carriers, which is not necessarily the same as the number of Ethernet lanes (m).

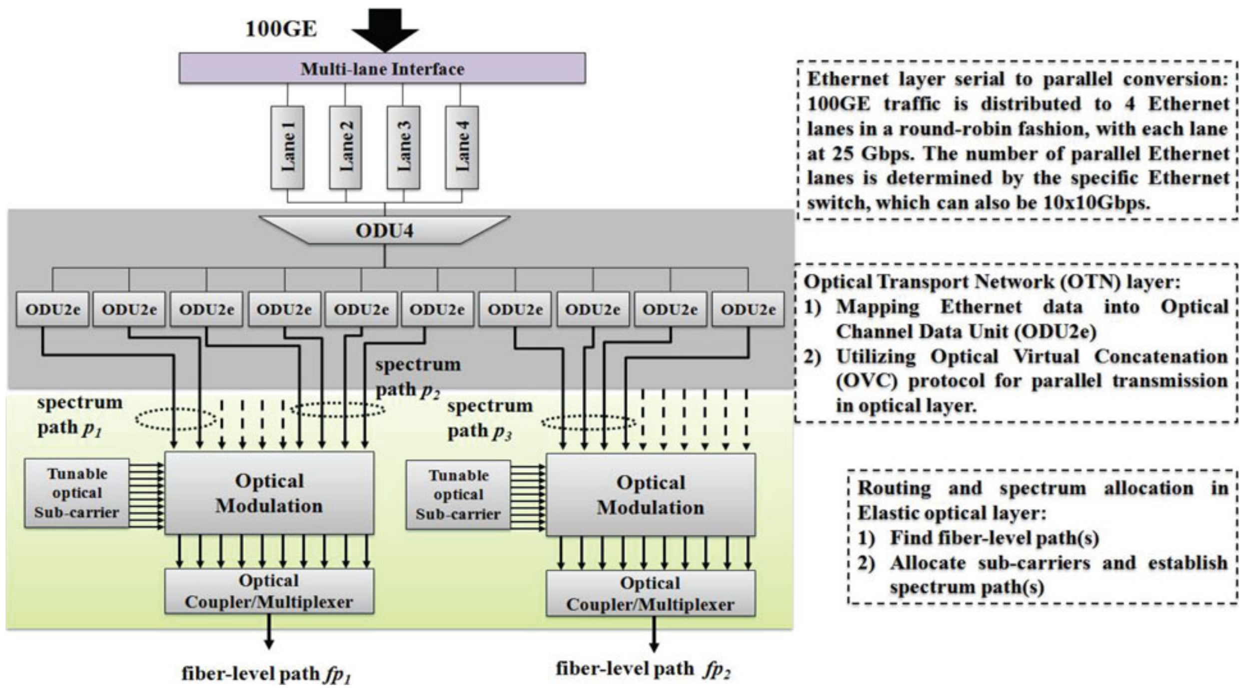

Fig. 1. Parallel transmission in elastic optical networks for 100 Gbps Ethernet.

100 GE, i.e., 4×25 Gbps and 10×10 Gbps. In our example, 100 GE signal is distributed into 4×25 Gbps lanes via MLD interface. OTN layer decides the size of optical channel data unit (ODU) based on the capacity of the sub-carriers. Assume each sub-carrier here can support an ODU channel (10 Gbps), traffic from an Ethernet lane at 25 Gbps can not be directly modulated onto a sub-carrier. An ODU4 channel is therefore used first, then inverse multiplexed into 10 ODU2e channels. After that, each ODU2e is mapped into optical channel transport unit (OTU2e) and modulated to a sub-carrier on a frequency slot. A group of consecutive frequency slots allocated to the connection is referred to as a spectrum path [3]. Here, the connection is established with three spectrum paths, i.e., p_1, p_2, and p_3. As it is illustrated, the spectrum paths can traverse different fibers, referred to as fiber-level paths. In Fig. 1, two fiber-level paths are used for this 100 GE connection, i.e., fp_1 and fp_2.

In this paper, we analyze the high-speed Ethernet system illustrated above and quantify the suitability of elastic (OFDM-based) optical networks to support Ethernet parallel transmission. Two issues are of particular interest: *spectrum fragmentation* and *differential delay*. Since all current routing and spectrum assignment (RSA) algorithms focus on allocating sub-carriers in a consecutive spectrum range, and don't take full advantage of parallel nature of elastic optical networks, the spectrum fragmentation can be significant. We show that optimizations can be used to reduce the spectrum fragmentation, and thus improve resource allocation effectiveness. Specifically, we show that the differential delay can be bounded within the limits defined in the current standards and commercial products.[2] This paper formulates a novel optimization model based on integer linear programming (ILP) and finds an optimal set of sub-carriers used in the parallel transmission, while minimizing overall usage of the optical spectrum. We also propose a heuristic algorithm to be applied in the scenarios where the optimization model becomes intractable. The numerical results show the effectiveness and high suitability of elastic optical networks to support high-speed Ethernet parallel transmission. To the best of our knowledge, it is the first investigation of the kind.

The rest of the paper is organized as follows. Section II gives a background overview. In Section III, we present the proposed ILP model and a heuristic algorithm. We show the numerical results in Section IV. Section V provides a literature review. We conclude the paper in Section VI.

II. Background

A. Key Technologies

The feasibility of parallel transmission concept stems from the inherent parallelism in the high-speed Ethernet, OTN-based as well as OFDM-based optical layers. The combination of the three concepts is ideal to facilitate parallelism in future high-speed transmission systems.

The Gigabit Ethernet transmission relies on duplex fiber cabling with one fiber deployed for each direction. The high-speed

[2]ITU-T G.709 [4] suggests that the realignment process has to be able to compensate a differential delay of at least ± 125 μs. In terms of commercial products, it has been reported that a commercial framer device can support 250 μs differential delay using internal memory and up to 128 ms differential delay using off-chip Memory [5], [6].

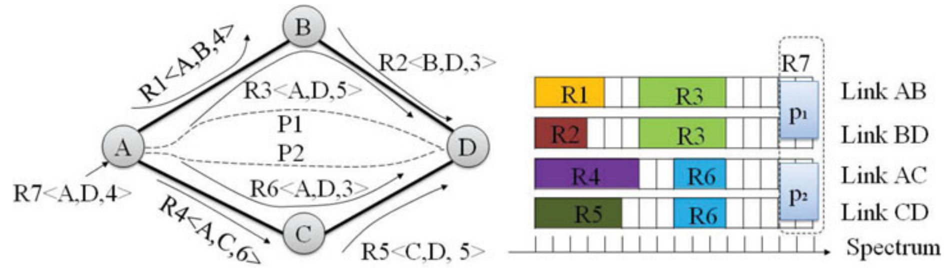

Fig. 2. An illustrative example of spectrum fragmentation and a solution with two spectrum paths.

Ethernet standard, i.e., IEEE 802.3ba, specified MLD to split high-speed serial Ethernet data into multiple virtual lanes in a round-robin fashion, as it was shown earlier in Fig. 1. As a result, the parallel optics systems are used in every Ethernet cabling solution. For instance, the 40 Gbps Ethernet calls for a solution of 12-fiber cabling, with each channel featuring four dedicated fibers for transmitting and receiving respectively, while saving the remaining four fibers as dark fibers for reliability [2].

In the optical layer, the built-in inverse multiplexing protocol in OTN, i.e., OVC, has been proposed to enable parallel transmission. As standardized in ITU-T G.709, OTN defines a set of *optical wrappers* with different sizes [7]. The client traffic is mapped into an optical wrapper of appropriate size and transmitted at corresponding line rates, referred to as OTUk. The OTN information structure supports line rates varying from approximately 2.5 Gbps ($k = 1$) to 112 Gbps ($k = 4$). Of note is that the OTN information structure has been recently updated in order to support the new emerging high-speed Ethernet services, in particular for 40 Gbps and 100 Gbps Ethernet. Two new optical wrappers are defined, referred to as, OTU3e2 (44.58 Gbps) and OTU4 (112 Gbps) respectively [4]. The technological maturity of OTN layer, including synchronization, error correction, framing and differential delay compensation, makes it well suited to facilitate parallel transmission.

In elastic optical networks, the so-called coherent optical OFDM (CO-OFDM) transponders can be used to realize elastic spectrum allocation required in the parallel transmission. The CO-OFDM transponders can be controlled by software to adapt to the spectrum path properties, including capacity per sub-carrier and modulation format [8]. This in turn enables an easy mapping between OTN wrappers and sub-carriers, as well as Ethernet parallel lanes.

B. Differential Delay in Parallel Transmission

In general, parallel transmission in OFDM-based networks falls under two categories: 1) single spectrum path transmission, 2) multiple spectrum paths transmission. In the first scenario, a single spectrum path utilizing a group of consecutive sub-carriers is set up for transmission. In the second scenario, data is split into multiple spectrum paths which can be allocated on the same or diverse fibers. In either category, sub-carriers experience different end-to-end delay, even when transmitted over the same fibers. For instance, in Fig. 1, the sub-carriers allocated to the spectrum paths, p_1 and p_2, can experience the delay difference resulting from imperfections in optical fibers. We distinguish two main types of differential delay: (1) fiber effects caused differential delay, and (2) path diversity caused differential delay.

1) Fiber Effects Caused Differential Delay: The main fiber effect to cause differential delay is the GVD due to the fact that sub-carriers on different frequencies travel (in form of waves) at different speeds.

An approximation of the maximum delay difference caused by GVD in a spectrum path is as follows:

$$\Delta d_{\max} \approx D(f_c) \cdot (f_{\max} - f_{\min}) \cdot L \quad (1)$$

where $D(f_c)$ is the fiber dispersion at the central frequency; $f_{\max}$ and $f_{\min}$ are the highest frequency and smallest frequency of the sub-carriers used by a spectrum path, see [9]; and L is the transmission distance. The condition of (1) is that the central frequency is much larger than $(f_{\max} - f_{\min})$. The OFDM-based optical networks follow the same spectrum dimension as *"fix grid"* [10], i.e., the central frequency is $f_c = 193.1$ THz, which is much larger than the frequency difference in any spectrum path. Hence, Equation (1) can be directly applied. As an example, we assume that 100 GE utilizes a spectrum path composed of 10 consecutive sub-carriers and also assume that each frequency slot is 50 GHz,[3] i.e., channel spacing is 0.4 nm. The fiber dispersion of an SMF is 17 ps/nm/km at the central frequency [9]. Hence, the maximum differential delay caused by dispersion in the parallel transmission is $\Delta d\max \approx 0.68\ \mu$s for a connection with physical distance of 1×10^4 km.

2) Path Diversity Caused Differential Delay: Another, and more commonly considered type of differential delay in parallel transmission is caused by the path diversity. When spectrum paths used in the parallel transmission traverse different fiber-level paths, the different transmission distance along different paths also leads to the differential delay. The differential delay caused by the fiber diversity can be simply calculated as L/v, where v is the signal propagation speed in the path and L is the path length. Considering the standard SMF where the signal propagation speed is 2×10^5 km/s, for a connection with length of 1×10^4 km, the maximum differential delay between spectrum paths would be 50 ms.

C. Spectrum Fragmentation

As previously mentioned, the bursty nature of Ethernet connection demands may exacerbate the so-called *spectrum fragmentation issue*. To better understand this problem, we show an

[3]A frequency slot is generally smaller than 50 GHz. Here, we use the standardized channel spacing, i.e., 50 GHz as an example.

example in Fig. 2, where optical spectrum on each fiber link is assumed to be sliced into 16 frequency slots, with one sub-carrier on each frequency slot. The traffic demand is defined as $R(S, D, T_r)$, where S, D and T_r denote source, destination, and the number of required sub-carriers, respectively. In this example, two sub-carriers are assigned as the guard-band (GB) (typically used to insulate the adjacent spectrum paths). As it can be seen in Fig. 2, the spectrum on all fiber links are fragmented after the allocation of six spectrum paths, i.e., R_1–R_6. Upon the arrival of R_7, the request is rejected, due to unavailable consecutive spectrum; in fact, under current network condition, any demand requesting more than three sub-carriers would be blocked, even though there are sufficient sub-carriers available in total. This phenomena is particularly pronounced in case of high-speed Ethernet services at 40/100 Gbps. As we claim, this issue can be effectively addressed by distributing Ethernet traffic into parallel spectrum paths. In the example shown, R_7 can be set up by utilizing two parallel spectrum paths, i.e., p_1 and p_2, with two sub-carriers per path.

D. Assumptions and Discussion

In this paper, we assume all sub-carriers have the same transmission rate. In OFDM-based optical networks, however, it has been shown that the capacity per sub-carrier can be adaptively managed by using different modulation formats for different transmission distances [11], [12]. Our previous study in [13], for instance, showed that distance-adaptive modulation formats can be applied in parallel transmission in OFDM networks. In this paper, however, we stay with the assumption that all sub-carriers have the same transmission rate. In practice, this assumption is necessary to simplify the mapping between OTN frames and sub-carriers. Also, the spectrum allocation in practical optical OFDM networks is constrained by the availability of transponders, see [8], which is a real-world constraint. In practical systems, the availability of transponders has to be included in the RSA by constraining the overall number of spectrum paths within the number of available transponders. In this paper, without loss of generality, we assume that there are sufficient transponders to support the spectrum paths, noting that practical systems need an additional constraint.

As previously discussed, the main factor of differential delay in parallel transmission is path diversity. Considering the same transmission distance, the differential delay caused by the GVD among sub-carriers is thus insignificant compared with the delay difference caused by propagation, e.g., 0.68 μs versus 50 ms. Therefore, we only consider the differential delay caused by path diversity in the evaluation. It should be noted that the optimization model can account for the fiber effects caused differential delay issue, which may become useful for new materials as they induce new fiber propagation properties. Finally, we assume that the differential delay is compensated in the OTN layer, due to the infeasibility of optical buffering.

III. Parallel Transmission Algorithms

A. Preliminaries

The notations are summarized in Table I. The following definitions are used:

TABLE I
NOTATIONS

Parameter	Description
$G(V, E)$	A graph represents an elastic optical network with nodes in set V and edges in set E
f_i	A sub-carrier with index i
s_f	The size of a frequency slot
F	An ordered set contains all frequency slots (sub-carriers) on a link, $F = \{f_1, f_2, ..., f_N\}$
F^e	A set contains available frequency slots on link e
LD_e	Delay of the link e
L_e	Length of link e
$R(S, D, T_r)$	A connection request. S, D and T_r are source, destination and required sub-carriers, respectively
GB	Guard-band
M	Maximum acceptable differential delay
p	Spectrum path
fp	Fiber-level path
$\mathcal{P}$	Set of all the spectrum paths computed for R
$\mathcal{FP}$	Set of fiber-level paths computed for R
K	Maximum number of fiber-level paths can be used, $\lvert\mathcal{FP}\rvert \le K$

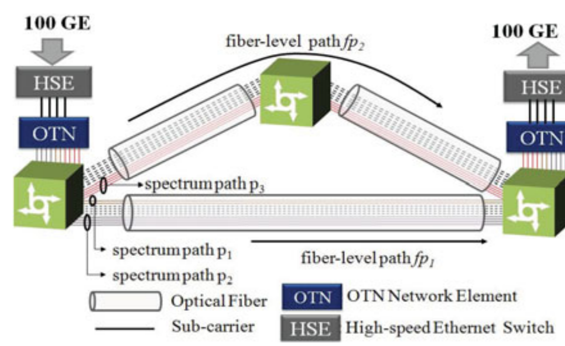

Fig. 3. Illustration of terminology.

1) *Sub-carrier* is a channel which carries signals in optical OFDM networks. Sub-carriers are orthogonal to each other and modulated to frequency slots with size of s_f.
2) *GB* is a slice of spectrum (expressed in sub-carriers) used to insulate two adjacent spectrum paths.
3) *Spectrum path*, denoted as p, is a spectrum slice allocated continuously from source to destination in form of a group of consecutive sub-carriers.
4) *Fiber-level path*, denoted as fp, is a physical route from source to destination, expressed in fiber links, over which one or multiple spectrum paths can be established.

Fig. 3 illustrates the terminology used, in line with the previous 100 GE example shown in Fig. 1. p_1, p_2 and p_3 are three spectrum paths. Two fiber-level paths are used: fp_1 and fp_2. The fiber-level path fp_1 contains two spectrum paths, p_1 and p_2, while fp_2 contains only one spectrum path p_3. The remaining notion can be taken from Table I. The variables used in the optimization are summarized in Table II.

B. ILP Optimization Model

The objective of ILP optimization model is to minimize the total spectrum resource along all spectrum paths established for a connection request, i.e.,

$$\text{Min} \sum_{p \in \mathcal{P}} \sum_{f_i \in F} \sum_{e \in E} x_{p,e,i} \tag{2}$$

subject to the following constraints.

Routing constraints: Equation (3) ensures that traffic on the spectrum path can be added and dropped only at source and destination nodes, respectively. Constraint defined in (4) guarantees that a spectrum path starts from the source node and ends at the destination node. Finally, Equation (5) eliminates loops at source and destination nodes.

$$\forall p \in \mathcal{P}, \tilde{v}, v \in V, v \neq s, d: \sum_{e=(\tilde{v},v) \in E} x_{p,e} = \sum_{e=(v,\tilde{v}) \in E} x_{p,e} \tag{3}$$

$$\forall p \in \mathcal{P}, \tilde{v} \in V, \tilde{v} \neq s, d: \sum_{e=(\tilde{v},d) \in E} x_{p,e} = \sum_{e=(s,\tilde{v}) \in E} x_{p,e} = x_p \tag{4}$$

$$\forall p \in \mathcal{P}, \tilde{v} \in V, \tilde{v} \neq s, d: \sum_{e=(\tilde{v},s) \in E} x_{p,e} = \sum_{e=(d,\tilde{v})} x_{p,e} = 0 \tag{5}$$

Spectrum continuity constraint: The spectrum paths are assumed to be all-optical which are restricted by the spectrum continuity constraints [14]. Equation (6) indicates that sub-carrier with index i is assigned to the spectrum path p from the source node. Equation (7) specifies that a spectrum path can only use sub-carriers with same index on all fibers it traverses.

$$\forall p \in \mathcal{P}, \tilde{v} \in V, \tilde{v} \neq s: y_{p,i} = \sum_{e=(s,\tilde{v}) \in E} x_{p,e,i} \tag{6}$$

$$\forall f_i \in F, p \in \mathcal{P}, \tilde{v} \in V, \tilde{v} \neq s, \tilde{v} \neq d, v \in V$$

$$\sum_{e=(\tilde{v},v) \in E} x_{p,e,i} = \sum_{e=(v,\tilde{v}) \in E} x_{p,e,i} \tag{7}$$

Spectrum consecutive constraints: For efficient modulation, a spectrum path utilizes consecutive sub-carriers [10]. The spectrum consecutive constraints are defined in (8) and (9). Equation (8) determines the number of sub-carriers allocated to spectrum path p. When two sub-carriers with index f_i and f_j $(j \geq i)$ are used for p, the right-hand side of (9) equals to T_p. This constraint ensures that the gap between two sub-carriers should be equal to or less than T_p. When f_i and f_j are not used at the same time, the right-hand side of (9) results in an infinite value, which keeps (9) true.

$$\forall p \in \mathcal{P}, e \in E, v \in V, f_i \in F: T_p = \sum_{e=(s,v)} \sum_{i} x_{p,e,i} \tag{8}$$

$$\forall f_i, f_j \in F, j \geq i, p \in \mathcal{P}, e \in E: f_j \cdot x_{p,e,j} - f_i \cdot x_{p,e,i} + 1 \leq Tp + (2 - x_{p,e,i} - x_{p,e,j}) \cdot \infty \tag{9}$$

Non-overlapping constraints: To avoid collision, a sub-carrier can not be assigned to multiple spectrum paths simultaneously. The binary variable $o_{p,p'}$ is defined to denote if two spectrum paths p and p' have at least one common link. The value of $o_{p,p'}$ is determined by (10) and (11).[4] When p and p' share at least one link, $o_{p,p'}$ equals to 1, otherwise it equals to 0. Equation (12) specifies that a frequency slot f_i can not be assigned to p and p' at the same time if two spectrum paths have common links, i.e., either $y_{p,i}$ or $y_{p',i}$ can equal to 1, but not both at the same, when $o_{p,p'} = 1$. Finally, Equation (13) defines that spectrum reservation and assignment only happens when a spectrum path p is used by the connection.

TABLE II
VARIABLES

Variable	Description
x_p	Binary variable; it equals to 1 if a spectrum path p is found for R; otherwise it is 0
$x_{p,e}$	Binary variable; it equals to 1 if a spectrum path p uses e, otherwise it equals to 0
$y_{p,i}$	Binary variable; it equals to 1 if a spectrum path p uses sub-carrier $f_i \in F$, otherwise it equals to 0
$x_{p,e,i}$	Binary variable; it is 1 if a spectrum path p uses sub-carrier $f_i \in F$ on link $e \in E$, otherwise it is 0
$o_{p,p'}$	Binary variable; it equals to 1 if spectrum paths p and p' share at least one link, otherwise it is 0
pd_p	Integer variable; it denotes delay of spectrum path p
T_p	Integer variable; it denotes the number of sub-carriers allocated to the spectrum path p
GVD_p	Integer variable; it denotes the differential delay caused by GVD on the spectrum path p

$$\forall p, p' \in \mathcal{P}, p \neq p', e \in E: x_{p,e} + x_{p',e} - o_{p,p'} \leq 1 \tag{10}$$

$$\forall p, p' \in \mathcal{P}, e \in E: o_{p,p'} \leq \sum_{e} x_{p,e} \cdot x_{p',e} \tag{11}$$

$$\forall p, p' \in \mathcal{P}, p \neq p', f_i \in F: y_{p,i} + y_{p',i} + o_{p,p'} \leq 2 \tag{12}$$

$$\forall p \in P, f_i \in F: x_p - y_{p,i} \geq 0 \tag{13}$$

GB constraint: The constraint defined in (14) specifies that the spectrum assignment only happens when the available sub-carriers are sufficient to meet the GB requirement. When f_i is allocated to a spectrum path p, a sub-carrier within the range $\{f_i - GB, f_i + GB\}$ cannot be allocated to other spectrum paths. In other words, all sub-carriers within the range $\{f_i - GB, f_i + GB\}$ are excluded from the available spectrum set of link e for other spectrum paths. Equation (15) ensures that a GB exists between two spectrum paths p and p', if they share at least one common link. When p and p' have no common links, $o_{p,p'}$ equals to 0, which guarantees that (15) is true.

$$\forall p \in \mathcal{P}, e \in E, \{f_i \pm GB\} \in F \setminus F^e: x_{p,e,i} = 0 \tag{14}$$

$$\forall p, p' \in \mathcal{P}, e \in E, f_i, f_j \in F:$$

$$|f_j \cdot x_{p,e,j} - f_i \cdot x_{p',e,i}| \geq GB \cdot o_{p,p'} \tag{15}$$

Bandwidth constraint: This constraint ensures that the number of sub-carriers assigned to all spectrum paths for R is equal to

[4] To linearize (11), we define a new binary variable denoted as $\gamma_{p,p',e} = x_{p,e} \cdot x_{p',e}$. The value of $\gamma_{p,p',e}$ is determined as follows: $\forall p, p' \in \mathcal{P}, e \in E$: $\gamma_{p,p',e} \leq x_{p,e}$; $\gamma_{p,p',e} \leq x_{p',e}$; $x_{p',e} + x_{p,e} - \gamma_{p,p',e} \leq 1$.

the traffic demand T_r,

$$\sum_{p \in \mathcal{P}, f_i \in F} y_{p,i} = T_r \tag{16}$$

Differential delay constraint: The maximum differential delay caused by the GVD is calculated using (1). Equation (17) defines $T_p \cdot s_f$ as the difference between the highest frequency and the lowest frequency of the sub-carriers allocated to the spectrum path p of length $\sum_e L_e \cdot x_{p,e}$.

$$\forall p \in \mathcal{P}, e \in E : GVD_p = D(f_c) \cdot s_f \cdot T_p \cdot \sum_e L_e \cdot x_{p,e} \tag{17}$$

Note that the constraint defined in (17) is non-linear. To linearize the constraint, we define an integer variable $z_{p,e}$, and $z_{p,e} = T_p \cdot x_{p,e}$, i.e.,

$$\forall p \in \mathcal{P}, e \in E : GVD_p = D(f_c) \cdot s_f \cdot \sum_e L_e \cdot z_{p,e} \tag{18}$$

Equations (19)–(21) determine the value of $z_{p,e}$ to be either zero or equal to T_p. The delay of p is defined in (22). The total differential delay is calculated in (23). The latter is bounded by the maximum acceptable differential delay M in the electronic layer (OTN).

$$\forall p \in \mathcal{P}, e \in E : 0 \le z_{p,e} \le x_{p,e} \cdot |F| \tag{19}$$

$$\forall p \in \mathcal{P}, e \in E : 0 \le z_{p,e} \le T_p \tag{20}$$

$$\forall p \in \mathcal{P}, e \in E : z_{p,e} \ge T_p - (1 - x_{p,e}) \cdot |F| \tag{21}$$

$$pd_p = \sum_{e \in p} LD_e \tag{22}$$

$$\forall p, p' \in \mathcal{P} : |pd_p - pd_{p'}| + (GVD_p + GVD_{p'}) \le M \tag{23}$$

C. Problem Size and Complexity

The proposed ILP model has an exponential complexity of $O(|P| \cdot (|P| + |E| \cdot |F|))$, where $|P|$ is the number of spectrum paths, $|E|$ and $|F|$ are number of links and sub-carriers, respectively. This makes the optimization model computationally expensive and practically intractable. Take a example of a network $|V| = 15$, $|F| = 16$, there are $|V| \cdot |V - 1| = 210$ node pairs. For each node pair, there are $|P| \cdot |F|$ instances of $y_{p,i}$. Assume four paths are used in the connection, i.e., $|P| = 4$, we have 13440 $y_{p,i}$ variables. Other variables can be calculated in a similar way. Thus, the total number of variables in the ILP model is rather high even for small networks.

The problem size can be reduced by pruning the variables. A common method used in the literature is to compute a set of paths in advance and use them as input to the ILP model. On the other hand, precomputed path solutions are limited and the complexity of the path computation in advance should also be taken into account in practical implementations.

D. Heuristic Algorithm

To make the proposed method more practically relevant, we propose a heuristic algorithm. The proposed algorithm decomposes the parallel transmission problem into two sub-problems, i.e., computation of fiber-level path(s) and spectrum assignment, as shown in Algorithm 1. The objective and all constraints of the proposed ILP model are also considered in the heuristic. To reduce the complexity, we limit that maximum K fiber-level paths can be used for a connection R.

Algorithm 1: RSA for Parallel Transmission

Input: $G(V, E), K, R(S, D, T_r)$
Output: One or multiple spectrum paths for R
Phase 1: Computation of Fiber-level Path(s)
while ($|\mathcal{FP}| \le K$) **do**
    while $destination(fp) \neq D$ **do**
        Select min-delay path fp from $\mathcal{S}$
        for *all nodes* v' *connected to* $destination(fp)$ **do**
            if (v' *not traversed in* fp) **then**
                create fp' by extending p to v'
                add fp' to $\mathcal{S}$
            end
            Put fp into $\mathcal{FP}$
            Remove fp from $\mathcal{S}$
        end
    end
end
Return $\mathcal{FP}$
Phase 2: Spectrum Assignment
//Step 1: Single spectrum path first;
for $k = 1$ *to* K, $fp_k \in \mathcal{FP}$ **do**
    Identify the spectrum path with maximum consecutive sub-carriers, i.e., p_k;
    if $F_{p_k} \ge T_r$ **then**
        A single spectrum path found; break;
    end
end
//Step2: Multiple Spectrum Paths
for $k = 1$ *to* K, $fp_k \in \mathcal{FP}$ **do**
    for *all* $e_i \in fp_k$ **do**
        Find spectrum paths on the fiber-level path fp_k and put in the path set $\mathcal{P}_k$
    end
    for $k = 1$ *to* K, $fp_k \in \mathcal{FP}$ **do**
        Sort all available spectrum paths in the increasing order of delay; and put in path set $\mathcal{P}$
        $N = |\mathcal{P}|$
    end
    for $k = 1$ *to* N **do**
        if $pd_{p_k} - pd_{p_1} \le M$ **then**
            $F + = F_{p_k}$
            if $F \ge T_r$ **then**
                Return spectrum paths and break;
            end
        end
    end
end

1) Computation of Fiber-Level Paths: The first phase of the proposed heuristic algorithm is to compute a set of fiber-level paths which is used as input to the spectrum assignment in phase 2 of Alg. 1. The algorithm starts from collecting all paths originating from source node s. All outgoing links from s are placed in a set denoted as $\mathcal{S}$ and sorted in an increasing order of path delay. The shortest path in $\mathcal{S}$, denoted as fp, is selected and extended to all the nodes connected to the sink node of fp, i.e., $destination(fp)$. Afterwards, the path set $\mathcal{S}$ is updated with the extended links and the shortest path from current $\mathcal{S}$ is selected. The same procedure is repeated till the shortest path in $\mathcal{S}$ reaches the destination node D. The computed path fp is placed in fiber-level path set $\mathcal{FP}$ and removed from $\mathcal{S}$. The algorithm continues to select the shortest path from the updated $\mathcal{S}$ and repeats the path computation. It breaks when no fiber-level path can be computed or K fiber-level paths have been computed. In the worst case scenario, the phase 1 of Alg. 1 has to visit all the nodes in the network to find a fp between S and D. Assuming the maximum node degree in the network is $\text{Deg}(V)$, the complexity of fiber-level path computation in phase 1 of Alg. 1 is $O(|V|^2 \cdot \text{Deg}(V) \cdot K)$.

2) Spectrum Assignment: In phase 2 of Alg. 1, the computed path set, i.e., $\mathcal{FP}$, is used as input. The algorithm attempts to find a single spectrum path as the solution first. It identifies the spectrum path with maximum number of consecutive sub-carriers on each fiber-level path $fp \in \mathcal{FP}$ and compares the available bandwidth with T_r. When it fails to find a single spectrum path solution, the algorithm attempts to compute a parallel transmission solution, i.e., by aggregating spectrum fragments from multiple spectrum paths. All spectrum paths are sorted in the increasing order of delay and put in the set P. Afterwards, the differential delay and bandwidth constraints are enforced. If the differential delay between a spectrum path $p_k \in \mathcal{P}$ and the shortest path $p_1 \in \mathcal{P}$ is not larger than M, i.e., $pd_{p_k} - pd_{p_1} \leq M$, p_k is included in the solution. Note that the GVD caused differential delay is not considered here. The algorithm outputs a solution when bandwidth requirement is satisfied. In the worst case scenario, the phase 2 of Alg. 1 has to check all the sub-carriers over all fiber links. Hence, the computational complexity of spectrum assignment phase is in order of $O(|K| \cdot |F| \cdot |E|)$.

IV. Performance Evaluation

In this section, we evaluate the performance of the proposed algorithms under dynamic traffic conditions. Connection requests arrive following a Poisson process with an average arrival rate of u and the holding time of each connection request follows the negative exponential distribution with an average value of h time units; thus the traffic load in the network is quantified as $u * h$ in $Erlang$. In our study, the mean inter-arrival time of the connection requests is 1 time unit and mean holding time is varied to achieve different traffic loads. In addition to traffic load in $Erlang$, we also use *network load* ($ErlangLoad * T_r$) in the evaluation for the fair comparison between connections with different bandwidth requirements (T_r). Blocking probability is used as a metric for assessing performance, which is defined as the percentage of blocked connection requests versus total connection requests. The ILP model is implemented in Gurobi Optimizer [15] and the heuristic algorithm is evaluated with an event-driven simulator in Java. We consider two representative values as the maximum acceptable differential delay, i.e., 250 μs as suggested in ITU-T G.709 [4] and 128 ms which can be supported by commercial framer/mappers [6].

A. ILP Model Evaluation

Due to the complexity of ILP optimization, we evaluate the proposed ILP model in a scaled-down network scenario using topology shown in Fig. 4. The number of sub-carriers per fiber link is 16; the maximum differential delay is 128 ms and GB is one sub-carrier. When the network is stable at a certain traffic load, a connection demand with bandwidth requirement between four and six sub-carriers is sent to a randomly selected source and destination pair and the ILP optimization is invoked. The same experiment is repeated 50 times.

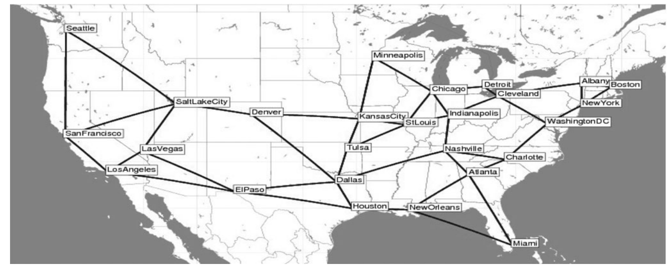

Fig. 4. US backbone network topology [16].

TABLE III
Connection Blocking Probability With the ILP Model and Heuristic (US Network Topology; M = 128 ms)

Load ($Erlang$)	Heuristic (K= 10)	Heuristic (K= 40)	ILP
30	16.0132%	8.0723%	0.000%
35	24.823%	10.419%	6.025%
40	34.392%	18.362%	14.025%
45	40.015%	22.753%	20.902%

Table III shows the percentage of blocked connections at each traffic load and compares the same scenario with heuristic. The heuristic is studied with $K = 10$ and $K = 40$. As there is no limitation in number of fiber-level paths used in the ILP evaluation, it seeks an optimal solution. It can be seen that ILP model always outperforms the heuristic algorithm when the problem is tractable. For instance, none of the connection requests is blocked using ILP model when traffic load is 30 $Erlang$. However, 16.0132% and 8.0723% connections are blocked using the heuristic algorithm with K =10 and $K = 40$, respectively. The reduction of blocking probability with a larger K is due to more spectrum paths available. With the increase of traffic load, the number of blocked connections increases with both the ILP model and the heuristic. However, the performance of proposed heuristic algorithm is getting close to the ILP model when the pre-computed paths are sufficient. For instance, the heuristic algorithm with $K = 40$ has around 22.753% blocking at 45 $Erlang$, whereas the ILP model leads to 20.902% blocking at the same traffic load.

This set of results shows that the proposed heuristic algorithm perform better with a larger set of pre-computed paths, as expected. In addition, the heuristic algorithm proposed can always find a solution in a reasonable time. At the same time, the ILP becomes intractable with increased traffic load or with an increased number of sub-carriers per fiber link.

B. Performance of the Heuristic Algorithm

In this section, we investigate the performance of proposed heuristic algorithm using the topology shown in Fig. 4. The

TABLE IV
SIMULATION PARAMETERS

F: number of frequency slots per link	128
GB: number of sub-carries as guard-band	0-3
T_r: number of requested sub-carriers	5,10,15, 20, 25, 30
K: maximum number of fiber-level paths	30
PT-1: with large M	$M = 128\ ms$
PT-2: with small M	$M = 256\ \mu s$

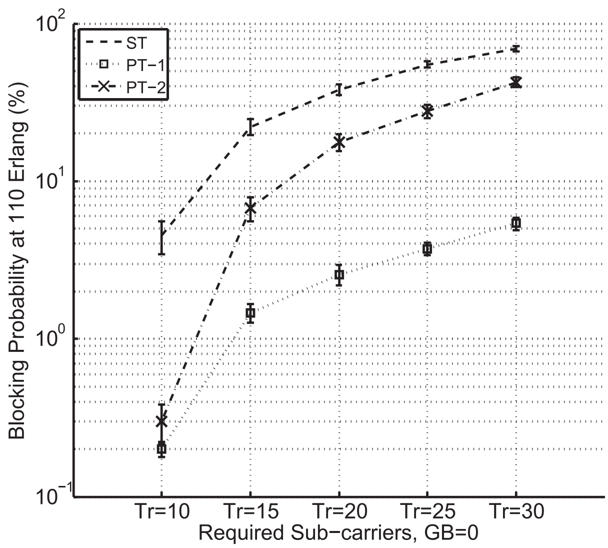

Fig. 5. Blocking probability versus T_r at 110 $Erlang$ (GB = 0).

simulation parameters are summarized in Table IV. The connection requests are uniformly distributed to the randomly selected source and destination pair. Approximate 20,000 connection requests are generated at every network load; every experiment is repeated 50 times to obtain an average value. The results in this section have a confidence interval of 95%. We distinguish between two parallel transmission scenarios:

1) *Parallel transmission on single spectrum path (ST)*: The required sub-carriers are allocated on the shortest spectrum path. Here, differential delay issue is not considered.
2) *Parallel transmission on multiple spectrum paths (PT)*: The required sub-carriers are not restricted to a single spectrum path. The parallel spectrum paths can be on the same or different fiber-level paths. The heuristic algorithm with maximum allowable differential delay 128 ms and 250 μs are denoted as PT-1 and PT-2, respectively.

1) Blocking Probability: Fig. 5 shows the blocking probability of different T_r at 110 $Erlang$ with $GB = 0$. It can be seen that using parallel spectrum paths for connection requests can reduce blocking probability, especially with large T_r. For instance, 20.9% connection requests are blocked with ST when $T_r = 15$. In comparison, only 1.4% connection requests are blocked with PT-1. Due to a stricter differential delay constraint, PT-2 has a higher blocking probability, i.e., 4.8%, comparing with PT-1. With the increasing spectrum requirements (in the number of sub-carriers), the reduction of blocking probability by using PT, especially with $M = 128$ ms, is significant. For instance, when $T_r = 30$, only 5.4% connection requests are blocked with PT-1, while 69.2% is blocked with ST. PT-2 also leads to a rather high blocking with $T_r = 30$ due to the strict differential delay constraint (42.3%). However, it is still lower than ST.

Fig. 6 shows the blocking probability of parallel transmission versus $ErlangLoad * T_r$ with $GB = 0$. It can be seen that parallel spectrum paths increase the acceptance ratio of connection requests. With increased bandwidth requirements, the blocking probability also increases. For instance, 1.8% connection requests are blocked with $T_r = 10$ when it is restricted to a single spectrum path (ST) at traffic load of 75 $Erlang$. With $T_r = 5$, maximum 0.9% connection requests with ST at 150 $Erlang$. Regardless of the number of required sub-carriers, parallel transmission always outperforms the single path counterpart. When network load is high, the performance of PT degrades, especially with higher connection granularities, and is comparable to single spectrum path performance, as seen in Fig. 6(b) and (c).

2) Impact of Differential Delay Constraint: In this study, we define PT-1 and PT-2 with maximum acceptable differential delay of 128 ms and 250 μs, respectively. As discussed in Section II-A, for a connection with length of 1×10^4 km, the maximum differential delay in a standard single mode fiber is only 50 ms. Hence, the differential delay constraint of PT-1 is sufficient to allow the allocation of the longest path in the network. This in turn implies that PT-1 can utilize longer paths than PT-2, which eventually leads to lower blocking probability (see Fig. 6). With the same experimental settings, e.g., $T_r = 10$ and 75 $Erlang$, blocking probability of PT-1 is 0.2% less comparing with PT-2. However, since PT-1 consumes more spectrum resources by using longer paths, and it will fail to find a solution for a request requiring large number of sub-carriers when network load is high. As shown in Fig. 6(c), the blocking probability of PT-1 is 0.4% higher than PT-2 when $ErlangLoad * T_r = 750$.

3) Impact of GB: Fig. 7 shows the performance of parallel transmission with different GB size. It can be seen that both PT-1 and PT-2 reduce blocking probability in comparison to ST. However, with increasing network load, the resource consumed by GBs in parallel transmission shows disadvantages. As shown in Fig. 7(a) and (b), PT-1 has the best performance when network load is low. When the network load is high, e.g., 75 $Erlang$ and 150 $Erlang$ with $T_r = 10$ and $T_r = 5$, respectively, both PT-1 and PT-2 have almost the same blocking probability as the ST. This is because most of the spectrum is used by GBs when the number of parallel spectrum paths is high. While PT-1 tends to reserve more resources by allowing for long paths, it has the highest blocking probability with $GB = 3$, as shown in Fig. 7(c). However, PT-2 has very strict differential delay constraint, i.e., 250 μs, it leads to the similar performance as ST with the increasing network load, since PT-2 can only find a single spectrum path under this network condition.

4) Spectrum Fragments Aggregation Ratio: As mentioned earlier, one of the benefits of parallel transmission is to aggregate sparse spectrum fragments. The more fragmented the spectrum, the more parallel spectrum paths need to be aggregated. To analyze this phenomena, we define a new performance metrics, called *Spectrum Fragments Aggregation Ratio*, as the percentage of connection requests served by multiple spectrum paths, which is mostly affected by the bandwidth requirements and differential delay constraints.

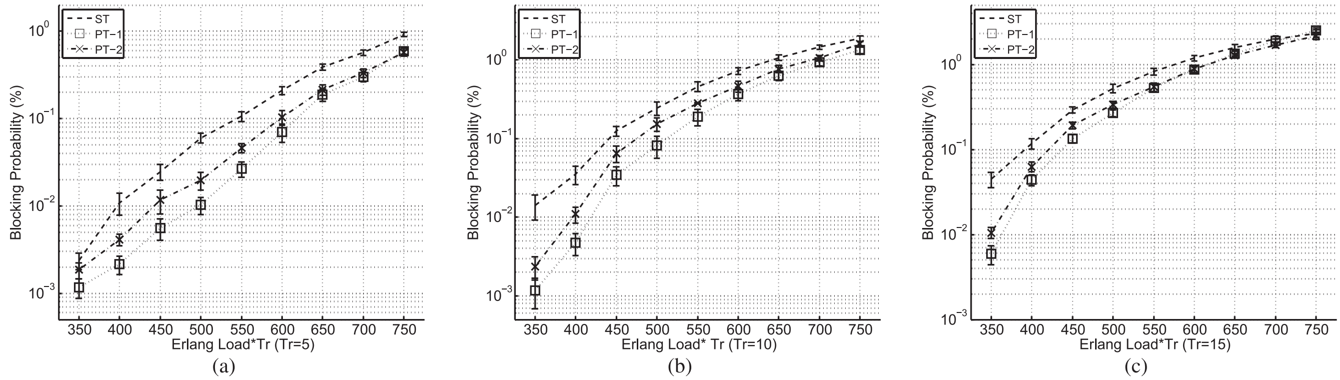

Fig. 6. Blocking probability versus network load (GB = 0).

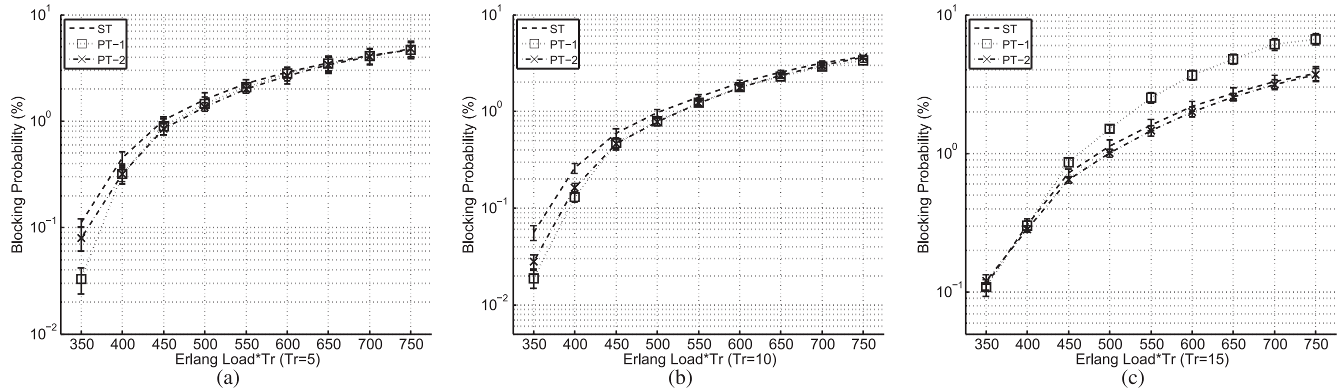

Fig. 7. Blocking probability versus network load (GB = 3).

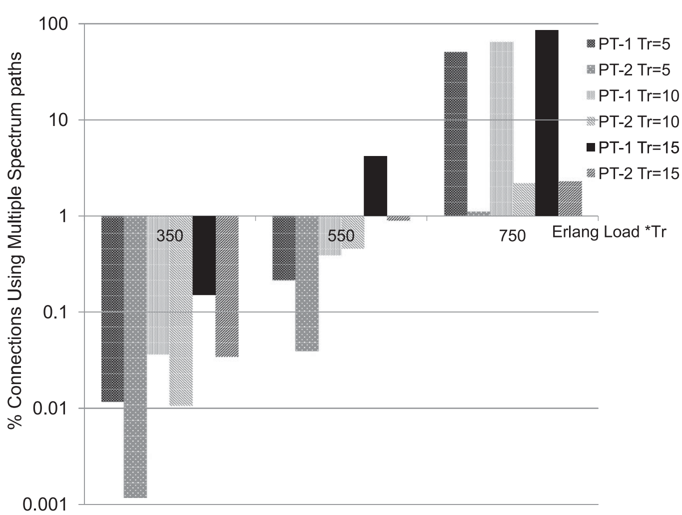

Fig. 8. Percentage of connections served with multiple spectrum paths versus $ErlangLoad * T_r$ (GB=0).

Fig. 8 presents measurements under three different network loads ($Erlang * T_r$). As it can be seen from Fig. 8, the differential delay constraint in PT-2 (250 μs) results in fewer connections using multiple spectrum paths. At low and medium loads ($Erlangload * T_r = 350$ and 550, respectively), most requests ($> 95\%$) are served with a single spectrum path and in the case of PT-2, the remaining requests are served mostly ($> 98\%$) using only 2 spectrum paths. In case of medium load ($Erlangload * T_r = 550$) with $T_r = 15$, PT-1 aggregates spectrum fragments more frequently comparing with PT-2. Around 55% connection requests are served with two spectrum paths and 25% connections are using three spectrum paths. 11% connections are set up with four spectrum paths and the others use higher number of spectrum paths. In case of PT-1, maximum ten spectrum paths were used.

This behavior is more pronounced at high network loads: the distribution of the requests served by multiple spectrum paths versus the number of spectrum paths used is presented in Fig. 9. As shown in Fig. 9, PT-2 uses only two spectrum paths for most connection requests, while a small fraction of connections using three spectrum paths. However, in the case of PT-1, as the requirement for spectrum slots increases, the fraction of connections using more spectrum paths also increases, with some connections also recorded using as many as 15 spectrum paths, each with a single sub-carrier. The unbounded nature of the number and length of the spectrum paths in PT-1 imply that algorithm can provision spectrum slots across disproportionately longer spectrum paths as compared to the single spectrum path only (ST). As a result, it leads to blocking of future connection requests, thereby degrading the performance at high network loads.

5) Impact of Network Topologies: Finally, we evaluate the parallel transmission in a different network, namely Abilene network with 12 nodes and 15 links [16]. Figs. 10 and 11 show

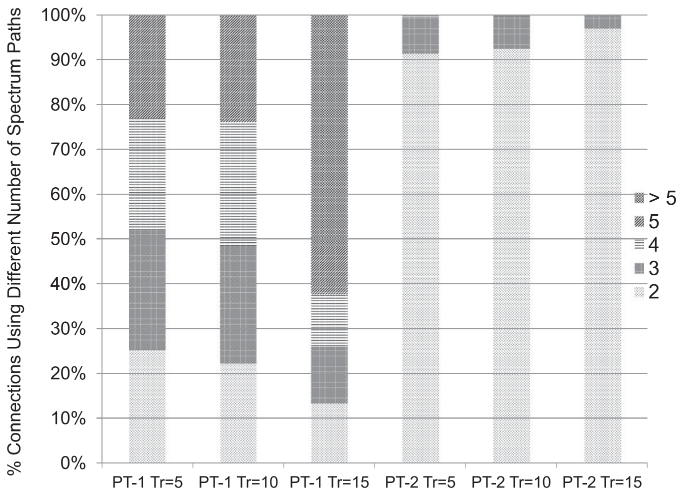

Fig. 9. Distribution of connections using different number of spectrum paths at $ErlangLoad * T_r = 750$ (GB=0).

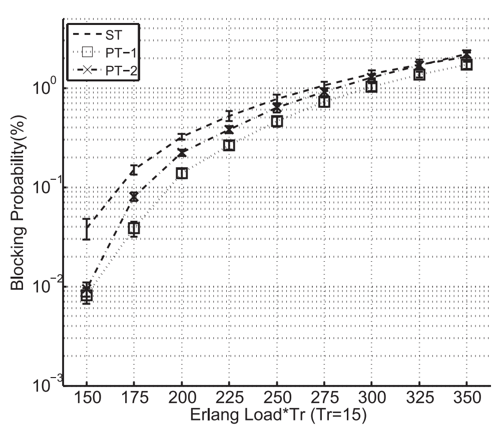

Fig. 10. Blocking probability versus network load, with no GB (GB = 0) in Abilene network.

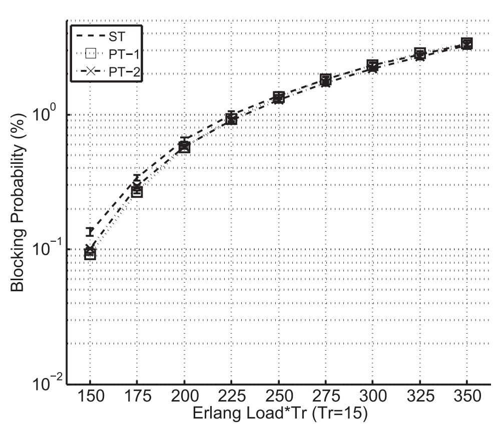

Fig. 11. Blocking probability versus network load, with a large GB (GB = 3) in Abilene network.

the blocking probability with $T_r = 15$. It can be seen that using multiple spectrum paths can reduce blocking probability in general. While the small network limits the maximum path length in PT-1, the larger acceptable differential delay leads to a better performance in terms of blocking probability. As shown in Fig. 10, PT-1 can reduce around 0.4% blocking probability comparing with ST at high network loads (e.g., $Load * T_r = 350$), while PT-2 has almost the same performance as ST due to the strict differential delay constraint.

V. Related Work

Since 2010, IEEE 802.3ba has standardized *parallel transmission* as the solution for high-speed Ethernet with ever increasing transmission rate which can be beyond 100 Gbps in the near future [2]. In particular, 100 GE has specified 10 parallel lanes, leveraging the mature 10 Gbps technologies in optical networks. To enable parallel transmission over wide area network, the International Telecommunication Union-Telecommunication Standardization Sector (ITU-T), has augmented G.709 OTN information structure for high-speed Ethernet at 40 Gbps and 100 Gbps [4].

It is not a coincidence that about the same time, the optical network have started to approach the so-called *optical capacity crunch*, where the capacities of single-mode fiber were shown to be reaching the Shannon limit in a few years from now [1], [17]. Optical parallel transmission was coined in [17] as the most promising solution for the optical capacity crunch. Optical spatial multiplexing and so-called *photonic multiple input multiple output* were proposed to explore the optical parallelism, which can multiplex multiple fiber strands or multiplexing multiple modes in a fiber [1].

In addition, optical networks are also shifting to improving spectral efficiency. It is known that conventional WDM networks have limit on the spectral efficiency. Therefore, it was nature for us to recognize that the inherent parallelism makes OFDM based optical networks a valid candidate for the high-speed Ethernet parallel transmission. Only by looking at early work *SLICE* proposed in [10], where optical spectrum is sliced into frequency slots, it can be seen that traffic is distributed to the parallel subcarriers, each utilizes one frequency slot (in parallel). However, so far none of the existing work has addressed the issues of high-speed Ethernet parallel transmission over elastic optical networks.

In [18], we presented an optimization algorithm for finding multiple spectrum paths in elastic optical networks applicable to the problems discussed in this paper. Also, optical parallel transmission in support of high-speed Ethernet was investigated in our past paper [19] for the first time, where an optimized parallel transmission framework based on OTN/WDM networks was proposed. Proposals have been presented also in [20] which presented a hybrid single path and multipath routing scheme for elastic optical networks. The authors proposed two heuristic algorithms, with consideration of path computation on the fly and usage of pre-computed paths. In [21], we have proposed a new scheme for high-speed Ethernet parallel transmission based on network coding which can simplify the traffic alignment and reduce buffer requirements in parallel transmission.

The present paper is different from the previous body of work, since it is an optimization framework for dynamic computations of parallel spectrum paths in elastic optical networks, with consideration of differential delay bounds within a spectrum path and also among the spectrum paths. Thus, the model is complete from the point of view of parallelization. Moreover, this paper is entirely focused on optical parallel transmission to support high-speed Ethernet. This paper, thus, for the first time, investigates the effectiveness and feasibility of using OFDM-based optical networks to support high-speed Ethernet in line with the current IEEE and ITU-T standards, widely accepted by the industry.

VI. Conclusion

Parallel transmission has been standardized in IEEE 802.3ba as the solution for high-speed Ethernet with ever increasing transmission rates. OFDM-based optical networks carry potential to support high-speed Ethernet due to its inherent parallelism. In this paper, we investigated the technical feasibility of parallel transmission in OFDM-based optical networks to support high-speed Ethernet and designed a novel framework which is in-line with current IEEE and ITU-T standards. We formulated an optimization model based on ILP for dynamic computation of multiple spectrum paths, with consideration of differential delay issue caused by path diversity and fiber effects. We also proposed an effective heuristic algorithm which can be applied when the optimization model becomes intractable. The numerical results showed that using multiple spectrum paths is especially effective in serving connection requests with high bandwidth requirements, regardless of GB size. It was also shown that differential delay issue is not an obstacle for practical implementation. In conclusion, the proposed parallel transmission framework can be used to effectively support high-speed Ethernet, while leveraging the maturity of lower-speed configurable optical technologies.

Acknowledgment

The authors would like to thank the Editor in Chief, Dr. P. Winzer, for his guidance in the paper revision phase. The authors also thank anonymous reviewers for their substantial and inspiring review comments. Finally, the authors would like to acknowledge Dr. W. Bziuk and M. Caria who dedicated considerable time to review the paper and provide constructive suggestions in the final revision.

References

[1] P. Winzer, "Optical networking beyond WDM," *IEEE Photon. J.*, vol. 4, no. 2, pp. 647–651, Apr. 2012.

[2] *Carrier Sense Multiple Access with Collision Detection (CSMA/CD) Access method and Physical Layer Specifications*, IEEE Std. 802.3ba, 2010.

[3] W. Shieh and J. Djordjevic, *OFDM for Optical Communications*. New York, NY, USA: Academic/Elsevier, 2010.

[4] "Interfaces for the optical transport network (OTN)," ITU-T Recommendations. (Feb. 2012). [Online]. Available: http://www.itu.int/rec/T-REC-G.709/e

[5] "Cisco SL-series." [Online]. Available: http://www.cisco.com/en/US/products/hw/modules/ps2710/ps5479/index.html

[6] "Intel ixf193 datasheets." [Online]. Available: http://www.datasheetarchive.com/ixf193-datasheet.html

[7] A. Gumaste and N. Krishnaswamy, "Proliferation of the optical transport network: A use case based study," *IEEE Commun. Mag.*, vol. 48, no. 9, pp. 54–61, Sep. 2010.

[8] J. López Vizcaíno, Y. Ye, and I. Tafur Monroy, "Energy efficiency analysis for flexible-grid OFDM-based optical networks," *Comput. Netw.*, vol. 56, no. 10, pp. 2400–2419, 2012.

[9] Y. Sun, T. Ono, A. Takada, and M. Tomizawa, "Wavelength-group-based optical virtual concatenation technique for data-intensive and latency-sensitive applications," in *Proc. IEEE Int. Conf. Commun. Workshop*, 2008, pp. 179–183.

[10] M. Jinno, H. Takara, B. Kozicki, Y. Tsukishima, Y. Sone, and S. Matsuoka, "Spectrum-efficient and scalable elastic optical path network: Architecture, benefits, and enabling technologies," *IEEE Commun. Mag.*, vol. 47, no. 11, pp. 66–73, Nov. 2009.

[11] K. Christodoulopoulos, I. Tomkos, and E. Varvarigos, "Elastic bandwidth allocation in flexible OFDM-based optical networks," *J. Lightw. Technol.*, vol. 29, no. 9, pp. 1354–1366, May 2011.

[12] M. Jinno, B. Kozicki, H. Takara, A. Watanabe, Y. Sone, T. Tanaka, and A. Hirano, "Distance-adaptive spectrum resource allocation in spectrum-sliced elastic optical path network," *IEEE Commun. Mag.*, vol. 48, no. 8, pp. 138–145, Aug. 2010.

[13] X. Chen, Y. Zhong, and A. Jukan, "Multipath routing in elastic optical networks with distance-adaptive modulation formats," in *Proc. IEEE Int. Conf. Commun.*, Jun. 2013, pp. 3915–3920.

[14] Y. Wang, X. Cao, and Y. Pan, "A study of the routing and spectrum allocation in spectrum-sliced elastic optical path networks," in *Proc. IEEE Int. Conf. Comput. Commun.*, Apr. 2011, pp. 1503–1511.

[15] "Gurobi optimizer." [Online]. Available: http://www.gurobi.com/

[16] "Sndlib." [Online]. Available: http://sndlib.zib.de/home.action

[17] P. J. Winzer, "Beyond 100G ethernet," *IEEE Commun. Mag.*, vol. 48, no. 7, pp. 26–30, Jul. 2010.

[18] X. Chen, A. Jukan, and A. Gumaste, "Multipath de-fragmentation: Achieving better spectral efficiency in elastic optical path networks," in *Proc. IEEE Int. Conf. Comput. Commun. Mini Conf.*, Apr. 2013, pp. 390–394.

[19] X. Chen and A. Jukan, "Optimized parallel transmission in OTN/WDM networks to support high-speed ethernet with multiple lane distribution," *IEEE/OSA J. Opt. Commun. Netw.*, vol. 4, no. 3, pp. 248–258, Mar. 2012.

[20] Z. Zhu, W. Lu, L. Zhang, and N. Ansari, "Dynamic service provisioning in elastic optical networks with hybrid single-/multi-path routing," *J. Lightw. Technol.*, vol. 31, no. 1, pp. 15–22, Jan. 2013.

[21] X. Chen, A. Jukan, and M. Médard, "A novel network coded parallel transmission framework for high-speed ethernet," in *Proc. IEEE Global Telecommun. Conf.*, Dec. 2013.

Xiaomin Chen received B.Sc. and M.Sc. degrees in telecommunications and information systems from Tongji University, Shanghai, China. She is currently working toward the Ph.D. degree at the Technische Universität Braunschweig. She has actively contributed to multiple EU and German projects. Her research interests include network optimization, parallelization, and high-speed Ethernet and optical technologies.

Admela Jukan received the Dr.tech. degree (*cum laude*) in electrical and computer engineering from the Technische Universität Wien, the M.Sc. degree in information technologies from the Politecnico di Milano, Italy, and the Dipl.-Ing. degree from the Fakultet Elektrotehnike i Racunarstva, Zagreb, Croatia. She is currently a Chair Professor of Communication Networks in the Electrical and Computer Engineering Department, Technische Universität Braunschweig, Germany. Prior to coming to Braunschweig, she was Research and Visiting Faculty at the Institut National de la Recherche Scientifique, University of Illinois at Urbana Champaign, and Georgia Tech. From 2002 to 2004, she served as a Program Director in Computer and Networks System Research at the National Science Foundation in Arlington, VA, USA. She has chaired and co-chaired several international conferences, including IFIP ONDM, IEEE ANTS, IEEE ICC, and IEEE GLOBECOM. She serves as a Technical Editor for *IEEE Communications Magazine*, and she is a co-Editor-in-Chief of the *Elsevier Journal of Optical Switching and Networking*. She is recipient of an Award of Excellence for the BMBF/CELTIC project "100Gb Ethernet" and was also awarded the IBM Innovation Award for integration of parallel computing and optical networking.

Ashwin Gumaste is currently the Institute Chair Associate Professor in the Department of Computer Science and Engineering, Indian Institute of Technology (IIT) Bombay. His recent work on Omnipresent Ethernet has been adopted by tier-1 service providers and also resulted in the largest ever acquisition between any IIT and the industry. This has led to a family of transport products. He has 20 granted U.S. patents. He has published about 150 papers in referred conferences and journals. He has received the DAE SRC Outstanding Investigator Award, the Vikram Sarabhai Research Award, IBM Faculty Award, PK Patwardhan Award, and the INAE Young Engineer Award.